JOURNAL OF MATERIALS SCIENCE 21 (1986) 1609–1614

Secondary phases and their role in the development of microdiscs on flux-grown $ErFeO_3$ crystal surfaces

P. N. KOTRU, S. K. KACHROO
Department of Physics, University of Jammu, Jammu 180001, India
B. M. WANKLYN
Clarendon Laboratory, Oxford University, Oxford, UK

The results of scanning electron microscope and qualitative element analysis studies, carried out on some typical structures exhibited by flux-grown $ErFeO_3$ crystals grown from PbO–PbF_2–B_2O_3 flux systems, are reported. Aluminium is present as an impurity in the crystals studied. Qualitative analysis of certain structures indicates the formation of magnetoplumbite ($PbO \cdot 6Fe_2O_3$) during the flux growth of $ErFeO_3$. Microdisc patterns are interpreted as resulting from the covering of such formations by the rapidly advancing growth fronts on the $ErFeO_3$ crystal surfaces. The crystallization of ErOF and $ErBO_3$ crystals on the $ErFeO_3$ crystal surfaces is also indicated by the qualitative analysis. Precipitation of the impurity phases during the flux growth of $ErFeO_3$ crystals and its effects on the development of the latter is discussed.

1. Introduction

Flux growth is the term used to describe the growth of crystals from molten solvents at high temperatures. It has the advantage of yielding crystals with habit faces which make them suitable for microtopographical investigations. Attempts to grow rare-earth orthoferrites have been reported by Remeika [1], Grodkiewicz and Nitti [2] and Wanklyn [3]. In order to characterize the surfaces and to understand the growth mechanisms of flux-grown crystals of $ErFeO_3$, the authors have carried out topographical studies. Kotru *et al.* [4] reported surface structures characteristic of $ErFeO_3$ crystals and concluded that defects in the form of misfit boundaries, tilted portions, microcrystals and cracks act as preferential sites for the nucleation of growth centres. SEM studies of some typical surface features of flux-grown $ErFeO_3$, $DyFeO_3$ and $YbCrO_3$ have been described by Kotru *et al.* [5].

In this paper, the authors present the results of a detailed study of some typical surface structures using qualitative element analysis and SEM.

2. Experimental details

The results reported here were obtained on $ErFeO_3$ crystals grown by the flux method from the composition 11.5 g Er_2O_3, 4.9 g Fe_2O_3, 1.2 g B_2O_3, 22 g PbO, 1 g PbO_2, 32.4 g PbF_2, pressed in a 50 cm^3 platinum crucible with a closely fitting lid. The charged crucible, on being kept at 1280° C for 4 h and then allowed to cool at 6° C h^{-1} down to 830° C, yields crystals of $ErFeO_3$. The separation of crystals from the flux is achieved by keeping them in 20% nitric acid under an infrared lamp. PbO_2 provides initially an oxidizing atmosphere so as to prevent attack on the crucible.

Typical features on the surface were studied using a scanning electron microscope (JEOL JSM–35CF), and qualitative elemental analysis was carried out using an energy-dispersive X-ray spectrometer (EDXS) attachment with a Cambridge Stereoscan (SU–10) scanning electron microscope.

3. Observations and discussion

3.1. Impurity phases

Fig. 1 is an electron micrograph showing narrowly as well as widely spaced growth fronts on a crystal surface. An interesting feature of this figure is the presence of certain microdisc patterns as shown at A and B. We shall come back to the finer details of these patterns later in the text. At the moment, let us consider a certain region of Fig. 1, taken at a higher magnification, displaying finer details of the region as shown in Fig. 2. One finds dot-like structures all along the edges of growth fronts. It is interesting now to know about these structures. The structure when examined at a still higher magnification under the SEM appears to be in the form of either black material projected above the surface or rounded cavities, as shown in Fig. 3. A survey of the entire region has revealed that the black structures or the cavities are hexagonal. The elevated black structures appear to be impurities precipitated during flux growth. The cavities may be due to the impurities becoming detached from the surface after their initial attachment. In order to confirm this and to know the type of impurities involved, qualitative elemental analysis was

0022–2461/86 $03.00 + .12

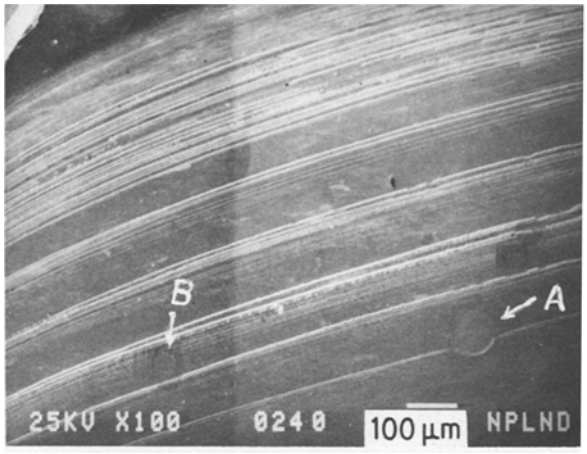

Figure 1 Electron micrograph showing non-uniformly spaced growth fronts, and microdisc formations as at A and B.

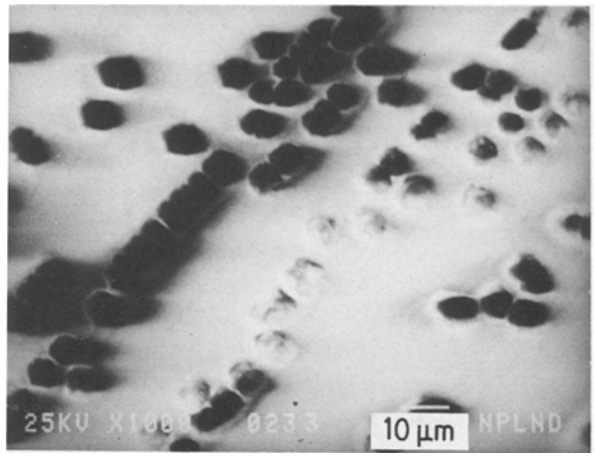

Figure 3 Enlarged view of some of the structures of Fig. 2, revealing them as of hexagonal shape.

carried out for regions of Fig. 3 using the EDXS attachment. Fig. 4 shows the analysis results recorded on the flat surface (general host surface) near to these structures (Fig. 4a), and also on these structures (Fig. 4b). The study of these spectra yields the following information:

1. The flat surface of $ErFeO_3$ has aluminium as an impurity.
2. The hexagonal black structures contain the elements aluminium, lead, iron and erbium. Comparison of the two spectra makes it abundantly clear that the black structures of Fig. 3 show the presence of lead, unlike the flat surface.

Traces of aluminium are present in the starting materials, but there is no doubt that the major source of aluminium is the sillimanite, Al_2SiO_5, muffle which contained the crucibles in the furnace. PbF_2 evaporates and reacts with Al_2SiO_5, forming a volatile species which enters the crucible. In this way both aluminium and silicon are transported into fluxed melts [6, 7]. Thus aluminium substitutes for iron in the growing orthoferrite crystal.

Kotru *et al.* [8] have reported that magnetoplumbite, $PbO \cdot 6Fe_2O_3$, crystallizes from fluxed melts used for obtaining orthoferrites or iron garnets. Lead is readily available from the flux (PbO–PbF_2–B_2O_3) used for the growth of these crystals. The black structures discussed above may, in all probability, be composed of this material. Its precipitation as a secondary phase during the crystallization of $ErFeO_3$ is expected. In addition it crystallizes as hexagonal plates or prisms.

In certain cases the impurity distribution has a kind of orderly arrangement, as is shown on the surface of a crystal in Fig. 5. It may be that the impurities being precipitated decorate the defects present in the crystal

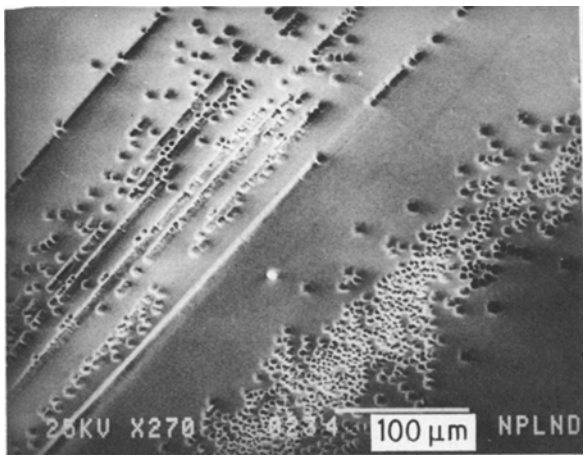

Figure 2 Scanning electron micrograph showing the tiny structures along the edges of the growth fronts of Fig. 1.

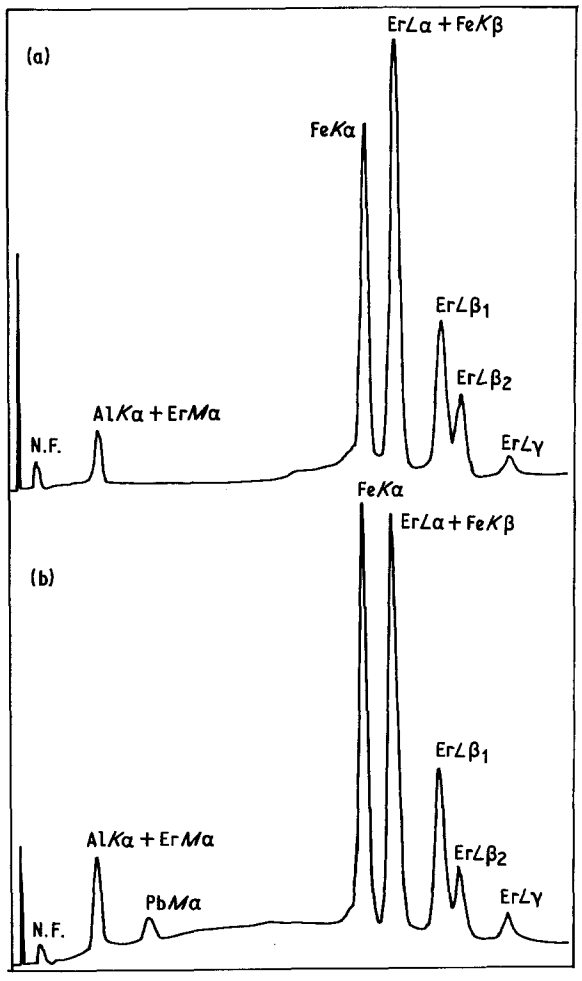

Figure 4 Energy-dispersive X-ray spectra recorded on (a) the flat surface of $ErFeO_3$, showing aluminium as impurity, (b) the black structures of Fig. 3 showing distinctive feature of lead as impurity.

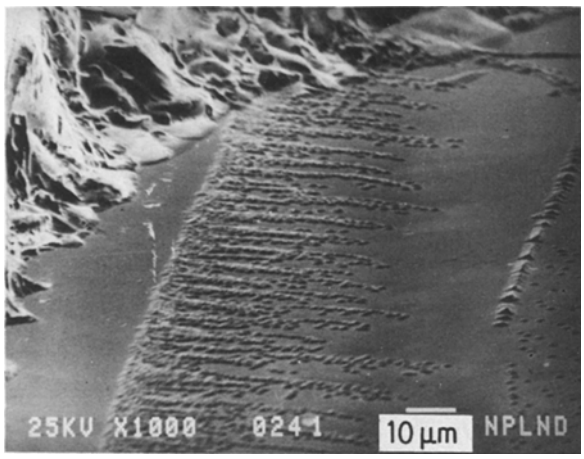

Figure 5 Scanning electron micrograph displaying arrays of impurities on the $ErFeO_3$ crystal surface when viewed obliquely.

(because of the extra energy available at these sites) and thus assume a kind of orderly distribution.

Fig. 6 is an electron micrograph showing a strip of white material with irregular structures on either side of it. Qualitative elemental analysis was carried out at three distinct places on this region. While the spectrum recorded for the black structures enclosed within the irregular structures is exactly the same as that recorded from the black structures of Fig. 3 (shown in Fig. 4b), the one recorded for the white strip is different. Figs. 7a and b are the spectra recorded on the flat crystal surface and the white strip of Fig. 6 respectively. From the study of these spectra, the following points emerge:

1. Aluminium, as an impurity, is present in both cases.
2. The Fe$K\alpha$ peak is significantly low (such a value could even be due to the background) in the case of the strip in comparison with the general $ErFeO_3$ crystal surfaces.

The above analysis confirms erbium to be the main metallic component of the white strip. It is impossible for erbium to be present as a metal in these systems since it is far too reactive. The strip could be crystals of ErOF or $ErBO_3$. Since the $ErFeO_3$ crystals have been cleaned in acid (HNO_3) the possibility of $ErBO_3$ is ruled out, as the borate would have dissolved. What we observe is probably therefore ErO_xF_{1-x}, which is usually called ErOF but is never quite stoichiometric. To further confirm this, the crystal was treated in acid (concentrated HNO_3) after recording the observation. The strip did not disappear, confirming that the strip is composed of ErOF rather than $ErBO_3$.

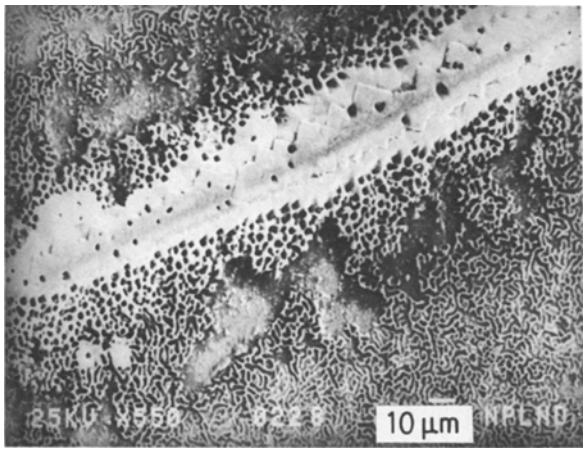

Figure 6 Electron micrograph showing a white strip surrounded on either side by irregular white linear structures enclosing black matter with in them.

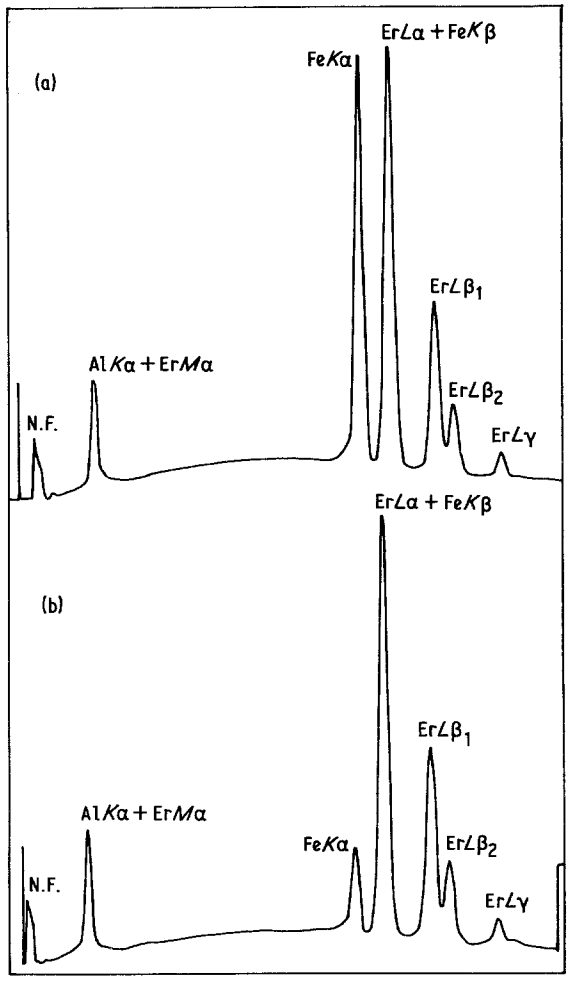

Figure 7 Energy-dispersive X-ray spectra recorded on (a) the flat crystal surface of $ErFeO_3$ near to the elevated structures of Fig. 6 showing aluminium as impurity, (b) the white strip showing a drop in the iron (Fe$K\alpha$) peak to a significantly low value in comparison with (a).

Isolated impurity overgrowths have also been observed on these crystal surfaces. Fig. 8 is an electron micrograph showing irregular elevated structures on an $ErFeO_3$ crystal surface. The texture of these structures is different from the rest of the surface, indicating their different compositions. To confirm this, several such regions were scanned under the SEM for elemental analysis. The study also revealed that erbium is the main component in these overgrowths.

The horizontal white line across Fig. 9a is the line along which the elemental scan was made. Fig. 9b is the element profile showing the distributions of iron and erbium as we scan from left to right. The two traces have been separated for convenience to avoid confusion due to overlapping.

The trace marked A corresponds to Fe$K\alpha$ and the trace B to Er$L\beta_1$. The traces clearly show that both iron and erbium are present on the general surface and

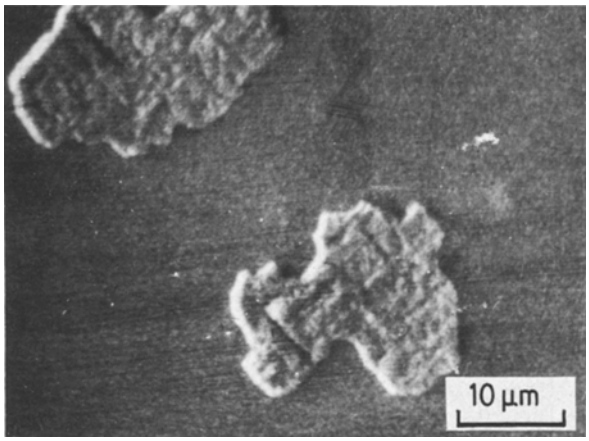

Figure 8 Electron micrograph of elevated irregular structures having a distinct texture on the $ErFeO_3$ crystal surface.

the two vertical bands (extreme left on Fig. 9a), whereas at the overgrowth region there is a sudden drop in the concentration of iron while the concentration of erbium continues. Wherever the overgrowth ends and exposes the general surface, the initial concentrations of erbium and iron are maintained in the trace. The profile thus indicates that erbium is the main component of these overgrowths. The overgrowths seem to be $ErBO_3$, which undergoes a structural transition on cooling, resulting in a very finely twinned structure which is hence opaque. On treating the crystal with concentrated HNO_3 it was observed that this overgrowth disappeared. This is expected as $ErBO_3$ dissolves in strong acids, unlike ErOF.

The spectra and element profile in Figs. 4, 7 and 9b (for Figs. 3, 6 or 8 and 9a, respectively) do not show the peaks of oxygen, fluorine or boron, though the evidence presented indicates the materials ErOF and $ErBO_3$, respectively. This is probably due to the fact that the analysis of light elements is particularly difficult [9]. With decreasing atomic number, the wavelengths of the characteristic X-rays become longer, the effect accelerating below about $Z = 10$. Thus for fluorine, oxygen, nitrogen, carbon, boron and beryllium ($Z = 9$ down to 4, respectively), their $K\alpha$ wavelengths increase in the order 1.8, 2.4, 3.2, 4.4, 6.8 and 11.3 nm. Such soft X-rays are also difficult to measure. As a result of this the sensitivity remains poor and, when there is also the fact that the basic X-ray yield is low for these light elements, it is not surprising that the expected elements oxygen, fluorine and boron are not detected.

It is significant to note that neither of these overgrowths, ErOF and $ErBO_3$, seem to have developed during the growth; instead they have developed at the end of growth. We established this by studying the surrounding features of a large number of such cases. There is no evidence of modification of growth fronts by these overgrowths. It was observed that the growth lines on the general surface had all the indications of continuity under the overgrowths. This is possible if the overgrowths take place after the growth of the $ErFeO_3$ crystal has ceased.

3.2. Microdiscs

Several investigators have observed circular microdisc patterns on different crystals [10–13]. All of them attributed the formation of microdiscs to protection of the surface by bubbles during the process of dissolution. However, the story is completely different in the case of the present observations.

We come back to the microdisc patterns as at A and B of Fig. 1. The edges of the growth fronts of Fig. 1 have magnetoplumbite impurities aligned along them as shown in Figs. 2 and 3. Our observations suggest that these magnetoplumbite crystals were precipitated

Figure 9 (a) Electron micrograph of an $ErFeO_3$ crystal surface showing two elevated vertical bands and an irregularly shaped overgrowth. The horizontal white line across the picture marks the line along which the elemental scans were made. (b) Element profile showing distributions of the elements iron and erbium as we go from left to right along the horizontal white line across (a). The traces marked A and B correspond to Fe$K\alpha$ and Er$L\beta_1$, respectively.

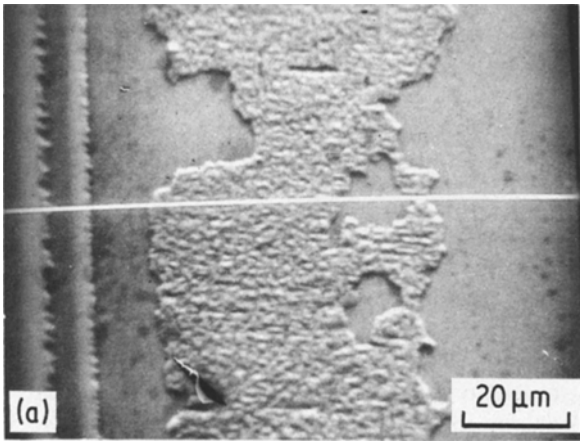

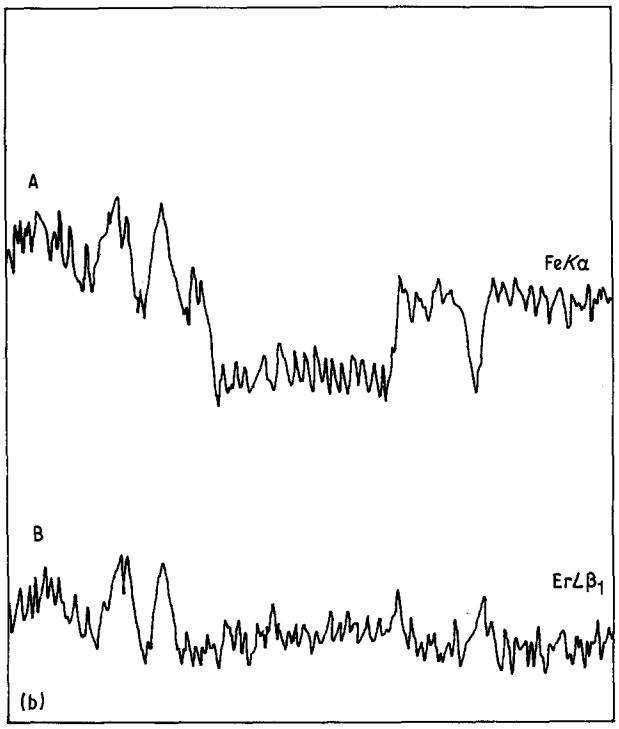

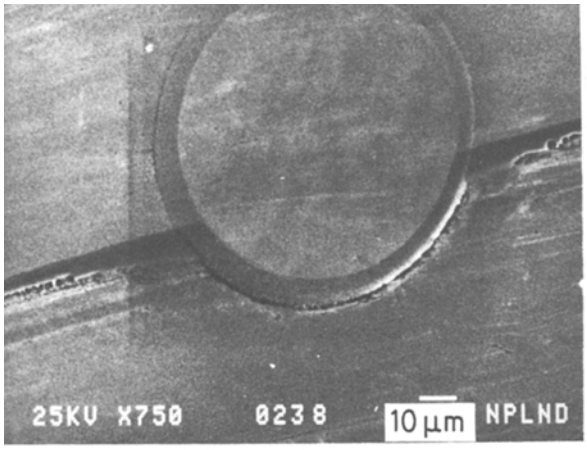

Figure 10 The microdisc A of Fig. 1 as viewed under the SEM at a higher magnification, revealing its structure and showing modification of approaching growth fronts by it.

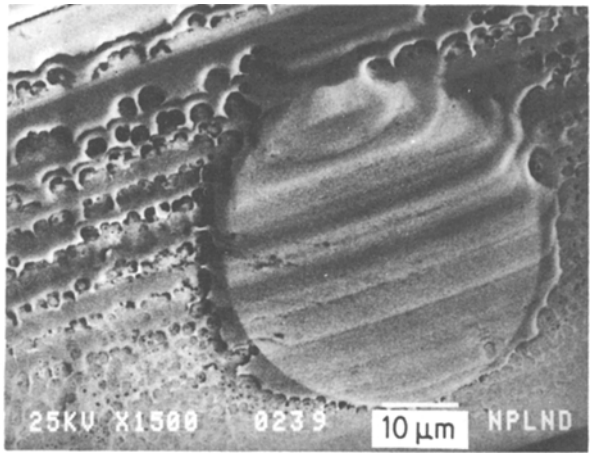

Figure 11 An electron micrograph illustrating microdisc B of Fig. 1 at a higher magnification, showing growth layers having crossed over it and surrounding impurities.

during the flux growth of $ErFeO_3$ and became attached to the growing surface of $ErFeO_3$ crystals. Such impurities, if attached to the host surfaces before growth had ceased, are bound to modify the advancement of growth fronts. The advancing growth fronts could also envelop these impurities if their attachment took place long before the growth had ceased, and get them incorporated into the crystal lattice as impurity inclusions. Such a covering process of impurity (magnetoplumbite) obstacles by rapidly advancing growth fronts from active initiation centres of growth may lead to the formation of elevated features on the surface, which could possibly be in the form of discs.

The elevated microdisc A of Fig. 1 is shown at a higher magnification in Fig. 10. The disc has an inclined periphery, and has a flat top with the base diameter bigger than that at the top. The disc has interacted with the advancing growth fronts, leading to their modification on encounter. This observation suggests the formation before the cessation of crystal growth. It is significant to note that the qualitative elemental analysis spectrum recorded on the top of this microdisc is the same as on the general {1 0 0} surface of $ErFeO_3$ crystals, suggesting thereby that the two are of the same composition. It is conjectured that the initial formation of the microdisc pattern is a result of the covering process of the impurities by rapidly advancing growth fronts on the $ErFeO_3$ crystal surface as explained above. Obviously, the subsequent deposition on the elevated microdisc structure has to have the same composition as the rest of the surface.

Fig. 11 represents an enlarged view of region B of Fig. 1, and shows a distinct process in the sense that the growth fronts have crossed over the disc thus modifying their advancement. In this figure one also observes a cluster of small-diameter circular patterns along the edges of growth fronts. Qualitative elemental analysis has confirmed that, while the material over the elevated microdisc is the same as that of the general crystal surface (similar to the trace in Fig. 4a), the material within the small circular patterns, aligned along the growth fronts and surrounding the microdisc pattern, exhibit a spectrum similar to that of Fig. 3 (see trace of Fig. 4b). Some of these circular patterns are elevations (attached impurities on the surface) while others are depressions (impurities having been separated at the end of growth). That in each case of these small circular patterns, there is evidence of modification of approaching growth fronts on encountering them, strongly suggests their formation before the cessation of growth. The same applies to the elevated microdisc pattern of Fig. 11, the cause of its formation being on the same lines as that of the microdisc of Fig. 10.

The extent and the mode of modification of an approaching growth front would depend upon the thickness of the growth fronts relative to the projection of an obstacle above the surface. In the event of the projection of the obstacle being greater than the thickness of the growth front, the latter is likely to be subjected to appreciable modification. If the obstacle is smaller, the growth front is likely to cross over it. The small obstacles have every chance of being enveloped by higher-speed growth fronts, and of finally getting embedded in the crystal as imperfections. The distinct difference in the process of modification of growth fronts by the disc of Figs. 10 and 11 is primarily on account of the thickness and greater number of growth fronts in the case of the latter.

The above observations are briefly summarized in Table I.

4. Conclusions

1. Using the $PbO–PbF_2–B_2O_3$ flux system for the growth of $ErFeO_3$ crystals results in the precipitation of $PbO \cdot 6Fe_2O_3$ (magnetoplumbites) as a secondary phase during growth.

2. Other secondary phases, ErOF and $ErBO_3$, also get precipitated but mostly at the end of the growth of $ErFeO_3$ crystals.

3. Engulfment of impurity phases precipitated during growth, by rapidly advancing growth fronts of $ErFeO_3$ on the growing $ErFeO_3$ crystal surface, may

TABLE I Features observed on $ErFeO_3$ crystal surfaces

Feature	Figure	Technique	Analysis	Conclusion	Further notes
General (flat) surface	Any figure	QEA*	Aluminium is present as impurity.	Aluminium is mainly transported from Al_2SiO_5 muffle by reaction of PbF_2 vapour. Aluminium goes in the $ErFeO_3$ lattice, substituting for Fe^{3+}.	Al$K\alpha$ peaks in all the qualitative element traces.
Dot-like structures	2, 3	SEM/QEA	Aluminium is present as impurity; lead, iron and erbium are also present.	Crystallization of impurity phase in the form of magnetoplumbite ($PbO \cdot 6Fe_2O_3$).	Most of them project above the surface; some are depressions.
Arrays of dot-like structures	5	SEM/QEA	As above.	As above.	Orderly arrangement suggests decoration of defects.
Irregular overgrowths	6	SEM/QEA	Besides aluminium, erbium is present as the main component. The features were not removed by strong HNO_3.	Impurity phase of composition ErOF likely.	–
Irregular overgrowths	8, 9	SEM/QEA	Erbium present as main component. The features were removed by HNO_3.	Crystallization of impurity phase of composition $ErBO_3$ likely.	–
Microdisc patterns	10, 11	SEM/QEA	Exhibit the same peaks in the QEA traces as the general (flat) surface of $ErFeO_3$.	Formed due to the process of covering over by $ErFeO_3$ of impurity phases during growth.	Growth fronts overlapping disc area. Modifications of growth fronts on meeting discs.

*Qualitative elemental analysis.

lead to the formation of microdisc patterns. The microdisc patterns, having the same elemental distribution as the general $ErFeO_3$ crystal surfaces, must have developed on the surfaces before the growth had ceased.

4. Aluminium is present as an impurity in all the $ErFeO_3$ crystals studied. It originates partly from traces of the impurity in the starting composition itself, but to a greater extent from the transport of aluminium into the crucible after reaction of volatile PbF_2 with the Al_2SiO_5 furnace muffle. It no doubt substitutes in the $ErFeO_3$ crystal lattice for Fe^{3+}.

Acknowledgements

Thanks are extended to Dr G. Garton, Head of the Crystal Growth Group, University of Oxford, for his encouragement in the collaborative research programme between the Physics department, University of Jammu and his laboratory. One of us (S.K.K.) is grateful to UGC (India) for the award of a Junior Research Fellowship. The authors thank Shri A. K. Razdan and Shri K. K. Raina for their help in the preparation of photographs. The research work forms a part of the project financed by the UGC. The help given by Shri V. G. Shah of the Physical Research Laboratory, Ahmedabad during SEM and EDAX work is gratefully acknowledged.

References

1. J. P. REMEIKA, *J. Amer. Ceram. Soc.* **78** (1956) 4259.
2. W. H. GRODKIWEICZ and D. J. NITTY, *ibid.* **49** (1966) 576.
3. B. M. WANKLYN, *J. Cryst. Growth* **5** (1969) 323.
4. P. N. KOTRU, S. C. GOSWAMI and B. M. WANKLYN, *J. Mater. Sci.* **18** (1983) 3729.
5. P. N. KOTRU, S. K. KACHROO, A. K. RAZDAN, K. K. RAINA and B. M. WANKLYN, *Bull. Elect. Micro. Soc. India* **7** (1983) 113.
6. B. M. WANKLYN and Z. HAUPTMAN, *J. Mater. Sci.* **9** (1974) 1078.
7. B. M. WANKLYN and G. GARTON, *ibid.* **9** (1974) 1378.
8. P. N. KOTRU, S. K. KACHROO and B. M. WANKLYN, *J. Mater. Sci. Lett.* **4** (1985) 1273.
9. T. D. MCKINLEX, K. F. J. HEINRICH and D. B. WITTRY (eds), The Electron Microprobe (Wiley, New York, 1966).
10. A. A. KUCHARENKO, Monograph on Ural Diamonds (exact title not known) (State Technical Publishing House, Moscow, 1950).
11. D. C. PANDEYA and S. TOLANSKY, *Proc. Phys. Soc.* **78** (1961) 12.
12. A. R. PATEL and K. N. GOSWAMI, *Proc. R. Soc.* **79** (1962) 848.
13. M. S. JOSHI and A. S. VAGH, *Physica* **30** (1964) 1757.

Received 28 May
and accepted 1 July 1985